Article:
Bateman, M.D., Bryant, R.G. and Luo, W. (2022) Getting the right age? Testing luminescence dating of both quartz and feldspars against independent age controls. Quaternary Geochronology, 72. 101366. ISSN: 1871-1014

https://doi.org/10.1016/j.quageo.2022.101366

Quaternary Geochronology 72 (2022) 101366

Contents lists available at ScienceDirect

Quaternary Geochronology

journal homepage: www.elsevier.com/locate/quageo

Getting the right age? Testing luminescence dating of both quartz and feldspars against independent age controls

M.D. Bateman [a,*], R.G. Bryant [a], W. Luo [b]

[a] Department of Geography, University of Sheffield, Winter St., Sheffield, UK
[b] Key Laboratory of Desert and Desertification, Northwest Institute of Eco-Environment and Resources, Chinese Academy of Sciences, Lanzhou, China

ARTICLE INFO

Keywords:
Barchan
Tsunami
Sampling
Single grain
Single aliquot

ABSTRACT

When luminescence dating was being developed much scientific effort was invested in showing it could achieve the correct ages, but this is now not routinely carried out for established protocols. This paper focussed on known age deposits from two case studies to explore whether correct ages were achieved. Case study 1 used the Storegga tsunami deposit dated to 8.2 ka sampled both horizontally and vertically and measured with OSL, IRSL and pIRIR. All results, for both quartz and feldspars, returned the correct age for the horizontal sample. Results from the vertical sample were more problematic with issues attributed to ongoing feldspar contamination of quartz and to beta heterogeneity. To agree with the independent age control single aliquot results required combination of >400 palaeodose replicates and in the case of IRSL the use of minimum age models. Measurements of feldspars at the single grain level using pIRIR measurements showed much improvement. Case study 2 used a barchan dune on the Tibet Plateau, China known to have been in position ~10 years. Both quartz and feldspars returned young ages close to the true age, but the feldspar ages with brighter luminescence signal were more accurate once the luminescence signal to background ratio was optimised. On the basis of this study we advise against sampling vertically. We also recommend measuring feldspars with single grain pIRIR where possible, measuring >150 palaeodose replicates per sample and choosing feldspars rather than quartz for very young samples.

1. Introduction

As luminescence dating has developed as a technique over the last 40+ years, there have been many studies which have tested the different stimulation approaches of thermoluminescence (TL), optically stimulated luminescence (OSL), Infrared stimulated luminescence (IRSL) and more recently violet stimulated luminescence (VSL) against independent age control (e.g. Nanson and Young, 1986; Balescu and Lamothe, 1994; Smith et al., 1997; Wallinga et al., 2001; Murray and Funder, 2003; Bateman et al., 2008; Briant and Bateman 2009; Kim et al., 2013; Ito et al., 2015; Ankjægaard et al., 2016). As methods to measure and analyse the palaeodoses (D_e) have developed researchers have compared them to results from older D_e protocols and with independent ages (e.g., Vandenberghe et al., 2004; Rodnight et al., 2006; Prescott et al., 2007; Roberts et al., 1999; Song et al., 2015). As time has passed and luminescence dating as a method has matured, there has been more of a standardisation of sample preparation, instrumentation, use of OSL on quartz and IRSL on feldspars, and most studies now measure D_e using the Single Aliquot Regeneration (SAR) protocol originally developed by Murray and Wintle (2000). Excluding Quaternary sediments at the upper limit of the technique or from challenging environments, when it comes to applying luminescence dating emphasis has moved to the generation of chronologies and whether these reflect true burial age, incomplete bleaching (e.g., Fuchs and Owen, 2008; Arnold and Roberts, 2009; Smedley et al., 2019) and/or post-depositional disturbance (e.g., Bateman et al., 2003; Bateman et al., 2007; Reimann et al., 2017).

The number of luminescence laboratories has rapidly expanded, and more scientists than ever are applying this dating technique. Periodic studies with independent age control can highlight how well routine approaches fair when dating material. This study examined a range of commonly applied luminescence measurement and analysis approaches to two known age samples. One was 8.2 ka in age (as dated by AMS radiocarbon) and well within the limits of luminescence dating and the other a very young sample (~10 years) which pushed the minimum limits of luminescence dating. In the former, sampling was varied to see the effects of vertical and horizontal sampling on age determination. This paper seeks to highlight how research decisions in sampling, measurement type and level influenced whether correct and

* Corresponding author.
E-mail address: m.d.bateman@sheffield.ac.uk (M.D. Bateman).

https://doi.org/10.1016/j.quageo.2022.101366
Received 23 November 2021; Received in revised form 19 May 2022; Accepted 8 June 2022
Available online 17 June 2022

independently verified ages could be determined. Where age inaccuracies were encountered this paper also seeks to illustrate when and where additional or alternative approaches are required.

2. Case study 1: storegga tsunami deposit, Montrose

2.1. Study site and sampling

The subsequent tsunami from the Storegga submarine landslide produced proximal waves in Norway >13 m and waves of 3–6 m as far away as Scotland, and eastern Greenland (e.g., Dawson et al., 1988; Smith et al., 2004; Bondevik et al., 2005; Wagner et al., 2010; Bondevik et al., 2012; Bateman et al., 2021). AMS radiocarbon has dated the Storegga tsunami to 8150 ± 30 cal years BP (Bondevik et al., 2012). As a single event, which is in the optimal time window for both the radiocarbon and luminescence techniques, the Storegga tsunami offers an ideal chronomarker against which to test luminescence dating. OSL has been successfully applied to tsunami deposits (e.g., Ishizawa et al., 2020; Shtienberg et al., 2020) and, whilst full bleaching may be an issue, Brill et al. (2012) showed for a recent (2004) tsunami deposit in Thailand unbleached residuals were low (~40 years). One of the few places where the Storegga tsunami sediments are exposed is in a basin edge bluff at Maryton on the southern side of the Montrose basin ~45 km north-east of Dundee, Scotland (Fig. 1). Here it is a ~15–20 cm grey, micaceous, silty fine sand with iron mottling found between low energy estuarine silty clays (Fig. 1B and C). Modelling and sedimentological analysis have shown this sediment was eroded and transported ~ 2 km by 3 waves up to 6.45 m high (Bateman et al., 2021).

Leighton et al. (2013) highlighted the need to carefully think about depositional environments and their stratigraphy when constructing a sampling strategy. The size, orientation and position within units can potentially affect the variability of sediment age and degree of bleaching sampled. As depicted in Fig. 2 horizontal sampling in theory should have both low chronological and depositional variability but if positioned badly may have targeted only poorly bleached sediment. In contrast, vertical sampling may contain sediment associated with multiple events and if partial bleaching did occur will include this. Sampling at Montrose tested this by collecting with a 5 cm diameter opaque PVC tube driven horizontally into the centre of tsunami sand (Fig. 1B; sample Shfd17230) and a second vertical core through the whole tsunami sand deposit. The latter was subsampled into ~1 cm slices and each slice separately prepared and measured (Fig. 1C; samples Shfd17232-Shfd17244).

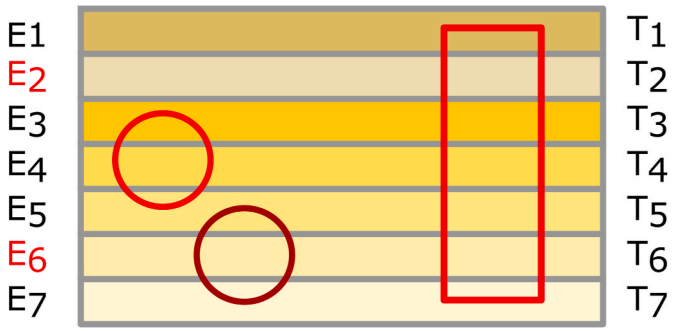

Fig. 2. Schematic of a horizontally bedded sediment unit comprising of multiple events (E_1-E_7) encompassing multiple time periods (T_1-T_7). Events in red are where only poor bleaching has taken place. The light red circle on the left shows sampling horizontally encompasses relatively few events/time periods so should have a low intrinsic age variability of grains sampled. The dark red circle whilst still encompassing few events is centred on a poorly bleach horizon. In contrast the rectangle on the right shows vertical sampling will encompass many events/time periods so should have a high intrinsic age variability of grains sampled and if poor bleaching is present will also include this.

2.2. Sample preparation and measurement

Given the aim of the paper, sample preparation followed widely adopted chemical and physical approaches to isolate grains in the 180–250 μm size range, clean them and separate out quartz and feldspar minerals (e.g., Bateman and Catt, 1996). All samples were measured in a Risø DA-15 reader with dual laser single grain attachment. Quartz and feldspar extracts were measured for both samples at the single aliquot (SA) level, with samples mounted as a ~2 mm diameter monolayer on

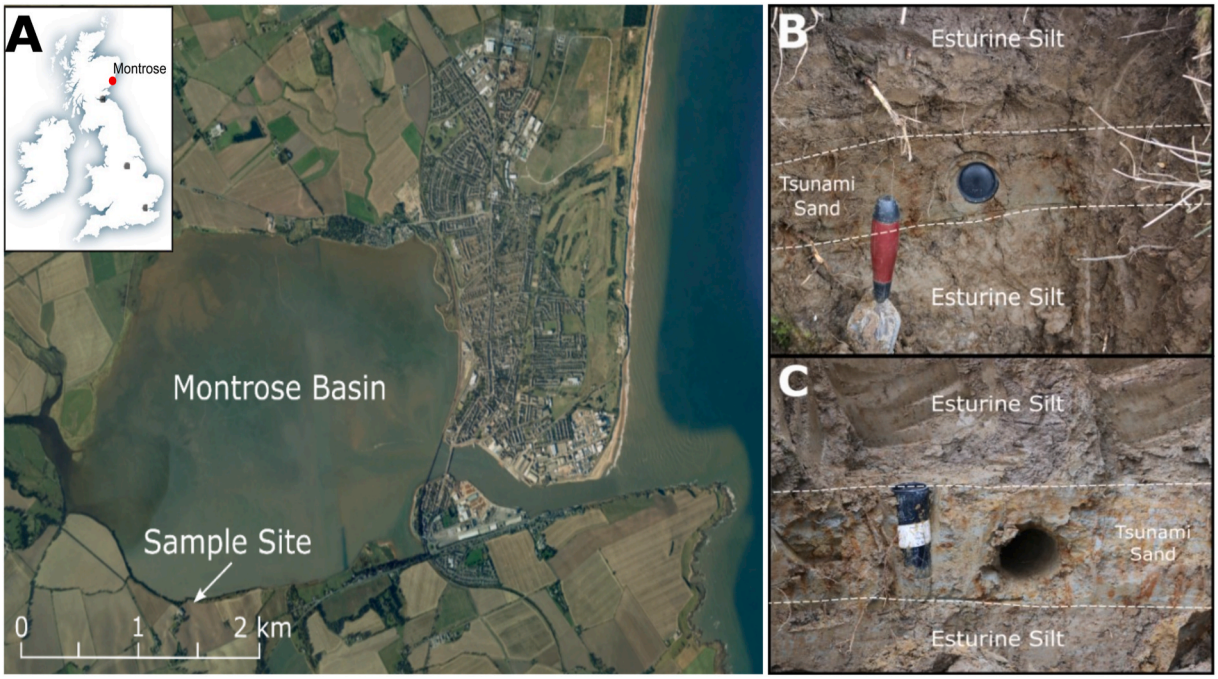

Fig. 1. Google Earth images of Montrose Basin, Scotland where Storegga tsunami deposits have been reported (e.g., Smith et al., 2004). (B) horizontal sample in centre of tsunami sand unit sampling only sediment from wave 2. (C) vertical sample through entirety of tsunami sand unit as deposited by all three waves.

9.6 mm diameter discs so that each aliquot contained ~ 90 grains. Single grain (SG) measurements were also made on the feldspar extracts.

Quartz SA OSL measurement was at 125 °C, with stimulation over 60s. Signal was measured through a Hoya U-340 filter and signal integrated from first 1.2s of stimulation with a background signal subtracted from an integral of the last 12s of stimulation data. An experimentally derived preheat of 180 °C for 10s was applied prior measurement. Measurement was with the Single Aliquot Regenerative (SAR) measurement protocol with five regeneration points (including zero and a recycled point; Murray and Wintle, 2000, 2003). Banerjee et al. (2001) recommended, prior to each OSL measurement within SAR, an IR wash at 50 °C to mitigate the effects of any feldspar contamination. As a result, a 40s IR at 50 °C was added to the SAR prior to each quartz OSL measurement at the SA level.

IRSL measured at 50 °C has been widely applied over a long period of time. However, anomalous fading is a widely recognised problem for feldspars (e.g., Mahan and DeWitt, 2019). To mitigate against this, post IR-IRSL (pIRIR) measurements at elevated temperatures have been developed (e.g., Buylaert et al., 2012; Rhodes 2015). Both IRSL at 50 °C and pIRIR at 225 °C were undertaken for this study. Single aliquot IRSL at 50 °C was measured to evaluate how well this approach measured a known age sample without fading correction. For this, IRSL measurement was at 50 °C with stimulation over 100s. Signal was measured through a BG3 and BG39 filter combination (Wallinga et al., 2000) and signal integrated from first 2s with a background signal subtracted from an integral of the last 20s of data. To see if IRSL at elevated temperatures performed better, pIRIR SG feldspar measurements followed a pIRIR protocol whereby after IRSL measurement at 50 °C a second IRSL measurement at 225 °C was made (e.g., Rhodes, 2015). In both cases stimulation was for 1s and signal integrated from first 0.06s with a background signal subtracted from an integral of the last 0.3s of data. IRSL measurements for both SA and SG were undertaken following a preheat of 250 °C for 60s as per Rhodes (2015) and used a SAR measurement protocol (Murray and Wintle, 2000, 2003) with five regeneration points. For SA measurements, between 48 and 96 replicate aliquots were measured for both OSL and IRSL to evaluate reproducibility. For SG, measurements continued until around 50 grains met the acceptance criteria of the recycling ratio 1 ± 0.2 of unity, recuperation <5%, error on the test dose <20%, naturally acquired signal significantly above background and SAR regeneration points well fitted by a growth curve.

External gamma dose rates were based on the field gamma spectrometry measurements measured with an EG&G micronomad. External beta dose rates were based on ICP-MS elemental measurements converted to dose rates using data from Guérin et al. (2011) and appropriately attenuated for grain size, density and a palaeomoisture value of 26% (based on present-day values; Table 1). For the vertical core beta dose rates were calculated for each subsample. The feldspar internal dose-rate assumed a potassium content of 12 ± 2% based on Lamothe et al. (1994). A cosmogenic dose rate contribution was calculated as per Prescott and Hutton (1994). As per a widely use approach, for samples with low overdispersion (OD) and normal D_e distributions, final D_e values used for age calculation were derived using the central age model (CAM) of Galbraith et al. (1999). Samples which had high OD values and skewed D_e distributions (e.g.Shfd17232-Shfd17244) had their D_e values for age calculation extracted using the minimum age model (MAM; Galbraith et al., 1999).

2.3. Results of horizontal v vertical sampling

At the SA level, the horizontal sample, whether measured with OSL or IRSL, had CAM D_e distributions that were normally distributed (Fig. 4) with low overdispersion (OD; 25 ± 3% for quartz and 23 ± 2% for feldspars; Table 1). Based on this data, and agreement between fast bleaching OSL and slower bleaching IRSL, the tsunami sediment was inferred to have been well bleached prior to burial and that the IRSL signal measured at 50 °C did not appear to have significantly faded. Quartz from the horizontal sample returned an age of 8190 ± 410 years and feldspar an age of 8480 ± 380 years comparing well to the independent radiocarbon age of 8150 ± 30 cal years BP. The subsamples extracted from the vertical core and measured at the SA level had D_e distributions that were more skewed (particularly for the feldspars), had larger OD values (21–47% for quartz & 19–42% for feldspars) and the down-core CAM and MAM D_e values were more variable (Fig. 3; Table 1). Five of the thirteen quartz SA OSL ages from the vertical core under-estimated true age (Table 1). The feldspar CAM derived SA ages measured with IRSL at 50 °C tended to overestimate the radiocarbon age (Fig. 3). Whilst this was improved when MAM D_e values were used for age calculation (with a sigma-b set at 0.1 to replicate well bleached sediments), some ages from subsamples still over-estimated the true age (Table 1). When SA D_e values from all samples of the vertical core were combined both CAM quartz (n = 500) and MAM feldspar (n = 497) gave SA ages of 8210 ± 380 years and 8000 ± 350 years respectively. These are concordant with the radiocarbon age.

In summary at the SA level, whether sampled horizontally or vertical luminescence ages concordant with the independent age could be

Table 1
Luminescence data for Storegga tsunami deposit at Maryton as measured by quartz OSL and feldspar IRSL at single aliquot level and pIRIR at single grain level. All D_e values unless indicated otherwise are CAM derived. Ages shaded in green are those within 1 standard error of the radiocarbon date of 8.15 ± 0.15 ka BP for this event.

Sample	Labcode	Depth (cm)	Dose Rate (Gy/ka)	n	OD (%)	D_e (Gy)	Age (ka)	n	OD (%)	D_e (Gy)	Age (ka)	Dose Rate (Gy/ka)	n	OD (%)	D_e (Gy)	Age (ka)
			Feldspar IRSL@50°C					Feldspar pIRIR@225°C				Quartz OSL@125°C				
Horizontal	Shfd17230	5-10	2.651±0.099	80	25	22.34±0.57	8.60±0.38	48	34	20.33±0.61	7.67±0.37	2.076±0.102	43	23	16.99±0.46	8.19±0.46
Vertical	Shfd17232	1	2.981±0.115	47	42	25.49±1.24*	8.55±0.53	36	52	22.16±0.83	8.26±0.42	2.145±0.118	49	27	18.7±0.61	8.72±0.56
Vertical	Shfd17233	2	2.981±0.115	47	32	22.26±1.83*	7.47±0.68	49	41	20.68±0.93	7.71±0.44	2.144±0.118	49	47	14.3±0.78	8.22±0.53
Vertical	Shfd17234	3	2.684±0.095	47	31	19.17±1.39*	7.14±0.58	49	29	20.91±0.63	7.79±0.36	2.069±0.088	40	21	17.37±0.55	8.40±0.45
Vertical	Shfd17235	4	2.688±0.095	48	30	23.21±1.38*	8.63±0.60	42	26	20.43±0.63	7.60±0.36	2.074±0.089	45	21	18.46±0.41	8.9±0.43
Vertical	Shfd17236	5	2.638±0.092	48	32	22.17±1.63*	8.40±0.68	52	25	20.18±0.51	7.65±0.33	2.023±0.085	44	33	15.63±0.68	7.72±0.47
Vertical	Shfd17237	6	2.637±0.092	48	19	27.64±1.66*	10.48±0.73	60	37	20.79±0.53	7.88±0.34	2.023±0.085	40	31	13.84±0.52	6.84±0.39
Vertical	Shfd17238	7	2.590±0.088	48	31	23.73±1.93*	9.16±0.81	32	56	34.32±3.01	13.25±1.24	1.976±0.081	47	20	18.23±0.55	9.23±0.47
Vertical	Shfd17239	8	2.544±0.085	47	24	26.18±01.73*	10.29±0.76	43	30	20.34±0.73	8.00±0.39	1.929±0.077	47	31	18.00±0.83	6.53±0.38
Vertical	Shfd17240	9	2.552±0.085	48	27	18.71±1.38*	7.33±0.59	50	28	19.74±0.67	7.73±0.37	1.937±0.085	44	34	12.6±0.52	6.50±0.39
Vertical	Shfd17241	10	2.622±0.089	48	24	21.45±1.38*	8.18±0.60	58	29	23.12±0.81	8.82±0.43	2.008±0.082	45	32	13.35±0.63	7.83±0.55
Vertical	Shfd17242	11	2.668±0.093	47	27	21.45±0.80*	8.04±0.41	56	35	23.35±0.72	8.75±0.41	2.053±0.086	46	41	10.84±0.41	5.28±0.30
Vertical	Shfd17243	12	2.640±0.092	48	24	20.74±1.44*	7.89±0.61	18	24	19.24±0.69	7.29±0.36	2.025±0.085	41	24	15.16±0.36	7.47±0.36
Vertical	Shfd17244	13	2.823±0.104	29	19	19.48±1.62*	6.90±0.63	-	-	-	-	2.209±0.098	32	24	15.16±0.36	7.69±0.52
Combined vertical							**8.00±0.35***				**8.01±0.31**					**8.21±0.38**

* D_e extracted with MAM

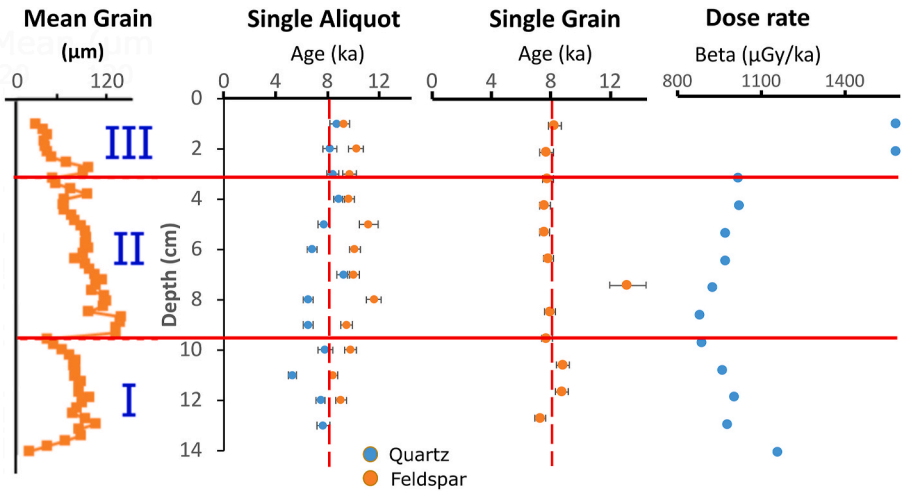

Fig. 3. Vertical core sedimentological, luminescence ages and dose rate data. For the luminescence measurements the core was split into 1 cm slices. Ages shown here are based on CAM derived D_e values although as discussed in the text MAM derived D_e values for SA feldspar measurements were used in final age calculations. Mean grain size measurements were taken every 2 mm with roman numerals indicating tsunmi each tsunami wave. For context mean grain size samples from over and underlying estuarine silt (not sampled for luminescence) are also shown.

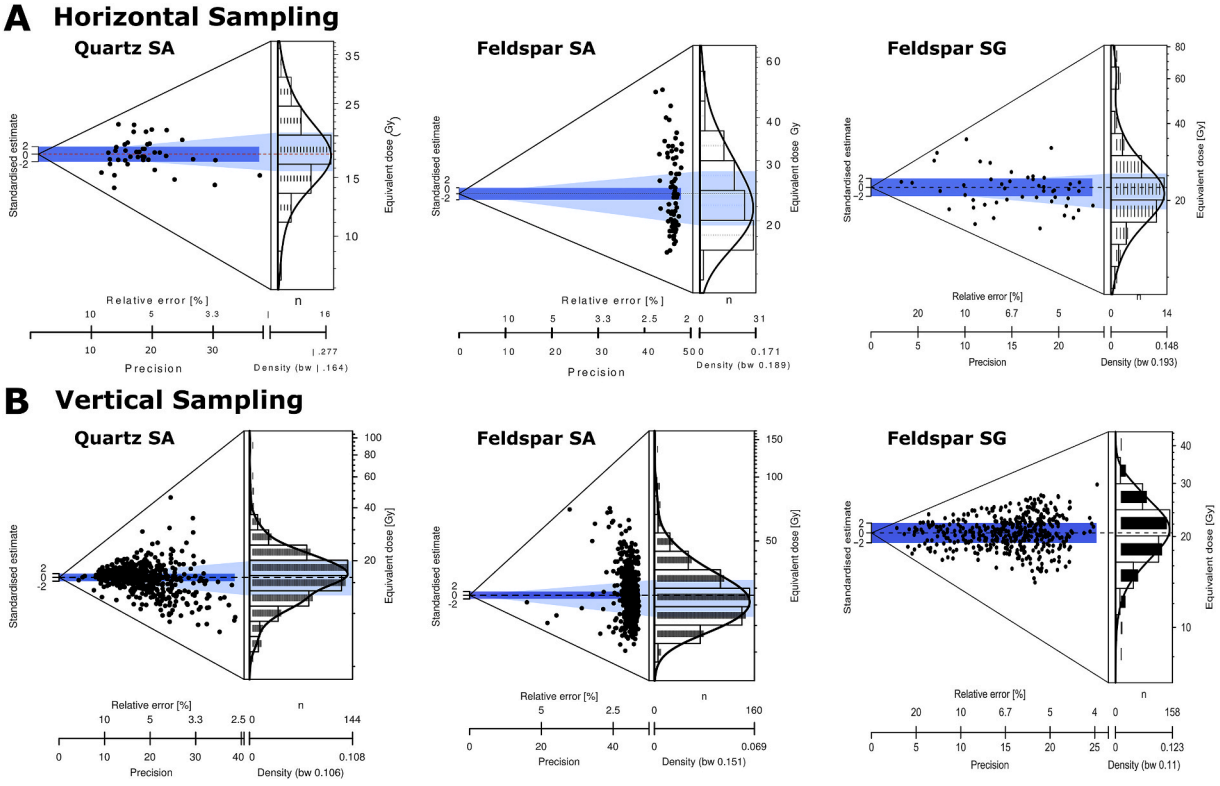

Fig. 4. Palaeodose (D_e) distributions for Montrose Storegga samples measured by quartz OSL and feldspar IRSL at the single aliquot (SA) level and by feldspar pIRIR at the single grain (SG) level. (A) Horizonal sample showing good reproducibility and low over dispersions for all methods. (B) Vertical sample (all data combined; n > 400) where SA reproducibility was lower and overdispersion higher. SG data showed good reproducibility and low overdispersion.

achieved although more careful statistical analysis and a higher number of replicates was required for the vertical sample to achieve this.

At the SG level both the horizontal sample and the vertical core subsamples had a bright feldspar signal (average natural signal ~15,000 cts/s^{-1}) with 90% of the feldspar SG signal coming from around 30% of the grains. Only between 200 and 400 feldspar grains per sample needed to be measured to get sufficient D_e data which met the quality assurance criteria detailed above. OD for feldspar SG measurements was high (25–52%) but D_e distributions were generally normally distributed apart from a few grains with much higher D_e values (Fig. 4). The horizontal sample returned a feldspar age of 7670 ± 370 years slightly younger than the independent age control of 8150 ± 30 cal years BP. For the subsamples from the vertical core, the feldspar CAM derived SG ages, with only one exception, all were within agreement of the independent age (Fig. 3; Table 1). When SG feldspar D_e data from all the vertical core samples were combined (n = 447) an age of 8010 ± 310 years was derived, concordant with the radiocarbon age.

In summary feldspars measured at the SG level, whether sampled horizontally or vertical, also produced luminescence ages concordant with the independent age. pIRIR measurements when compared to the IRSL measurements reduced variability between the subsamples taken from the vertical core (apart from one subsample with a large overestimation), required no selection of MAM model for D_e calculations and were closer to the true burial age.

3. Case study 2: barchan dune, Tibet Plateau

3.1. Study site and sampling

Luminescence dating very young sediments (younger than a few centuries) can be challenging as little time has elapsed for the luminescence signal to accumulate above background and growth curves can be sub-linear (Aitken, 1987). Cunningham et al. (2011) successfully applied OSL to 18th century storm deposits, whilst recently Bateman et al. (2018, 2021) applied quartz OSL to dunes less than 150 years old.

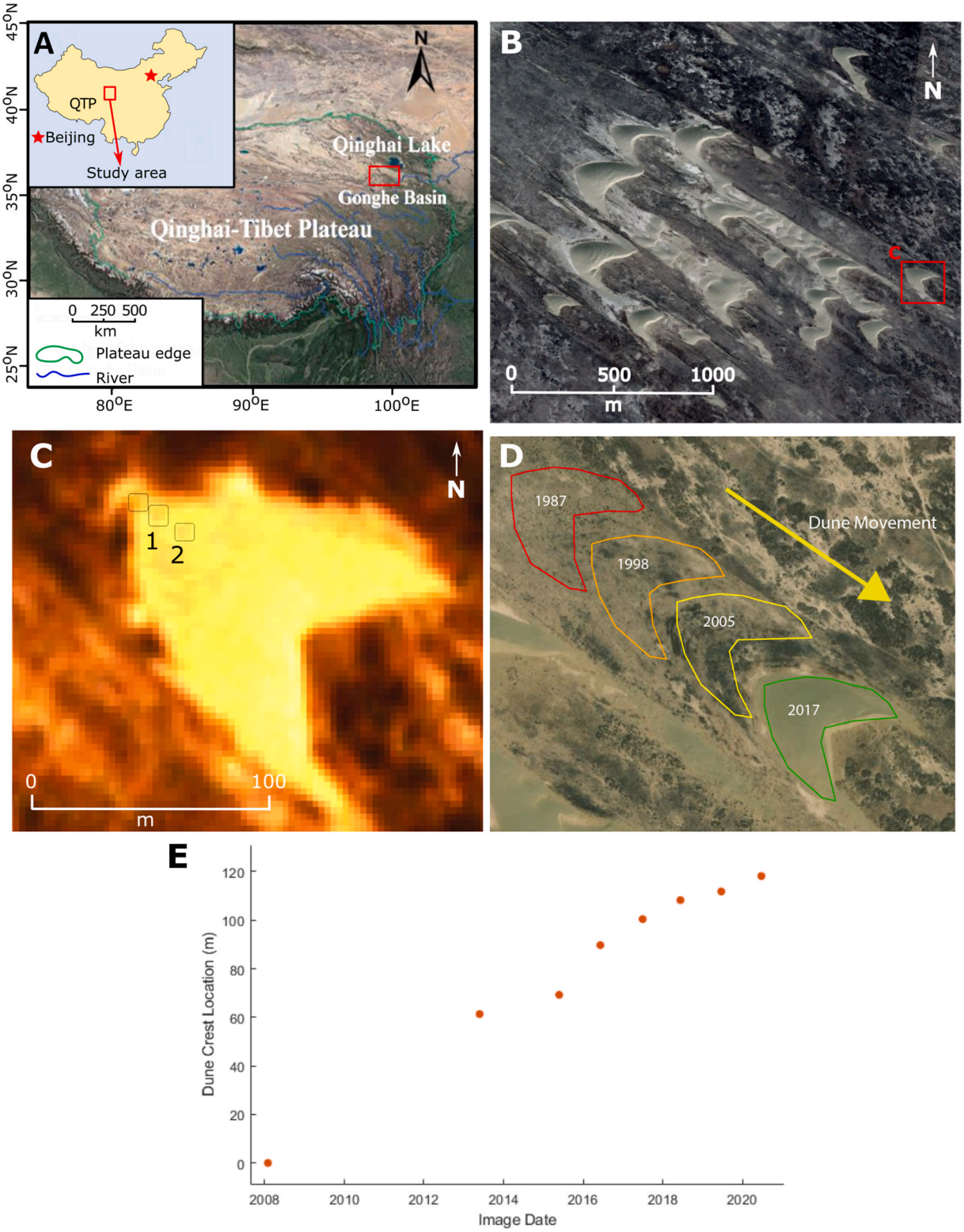

Fig. 5. Barchan dunes, Tibet Plateau. (A) Gonghe Basin study area within Tibetan Plateau. (B) Fast moving barchan dunes moving south-eastward. (C) Orthorectified PlanetScope false colour image (3 m pixel) of studied barchan with sample sites 1 and 2 shown. (D) Studied barchan position in 1987–2017 based on Landsat images overlain on a 2017 Google Earth image. (E) Barchan crestal position relative to 2008 extracted from analysis of Landsat and PlanetScope/Maxar imagry.

As earth surface monitoring by satellite has now taken place for over 50 years (Landsat 1 was launched 1972), exact age of fast-moving geomorphological features such as dunes can be established making them an ideal test for how well luminescence ages do when dating very recent sediment burial.

The Qinghai Gonghe basin is in the northeast of the Qinghai-Tibet plateau, China within which are significant areas of active dunes and wind eroded mega-blowouts (Fig. 5; Luo et al., 2019a, 2020; Qi et al., 2021). Dating of the latter shows these started to form only a few hundred years ago (Luo et al., 2019b). Sampling took place on a barchan about 100 m in length near a building which enabled ease of satellite geo-referencing. A 1985 image showed the whole dune was further to the north-west of its current position so no sediment contained within at its current position could be of that age, i.e., all sediment in the current dune should be < 35 year old (Fig. 5D). Analysis of a sequence of eight high-resolution PlanetScope and ESRI Basemap data [via Maxar, DigitalGlobe] of the study site (2008–2021: Fig. 5E), allowed a detailed understanding of dune movement as per Bryant and Baddock (2021). The Landsat and PlanetScope/Maxar time series data gave crestal migration rates of ~12 m and 8–9 m per year respectively. During barchan migration, sand from the tail of the dune is eroded and deposited down the dune slip face meaning that the oldest preserved buried sediment should always be found near the tail and the youngest on the slip face (Fig. 6). With the migration rates (as measured above), complete dune turnover (i.e., one wavelength of ~100 m) would have occurred in 9–11 years. As a result, the sediment buried in the dune tail should only be 10 years old. Two shallow test pits were dug into the presumed oldest sediment in the tail of the dune (Fig. 5C) from which two samples were collected.

3.2. Sample preparation and measurement

Sample preparation and instrumentation was as above for quartz and feldspar. SA measurement used 2 mm diameter aliquots with measurement of twenty-four replicates of each sample. In this case study quartz SAR incorporated eight regeneration points, an experimentally derived preheat of 160 °C for 10s and used a 40s OSL stimulation at 125 °C (shorter than case study 1 as a weaker signal decaying to background quicker was expected). IRSL SAR measurements also included eight regeneration points, were undertaken at 50 °C with a preheat of 250 °C for 60s and no fading corrections were attempted. The SAR data for both quartz and feldspar used an integral of the initial 0.8s as signal and an average signal of the last 8 s as background to produce growth curves and derive D_e values. External dose rates were based on ICP-MS elemental measurements converted using data from Guérin et al. (2011), a palaeomoisture value based on present-day values and a cosmogenic dose rate calculated as per Prescott and Hutton (1994). The feldspar internal dose-rate was based on a potassium content as measured by ICP-MS of 9.8 ± 2%. Whilst D_e replicates were normally distributed, OD was higher than might have been expected for dune sediments. This was due to 1–2 aliquots in each measurement dataset having 1–4 Gy D_e values which were much higher than the rest of the data which clustered just above 0 Gy. These high D_e aliquots were excluded as outliers from subsequent analysis. As some aliquots returned negative values, final D_e values for age calculation purposes were derived using the unlogged central age model (CAM) of Galbraith et al. (1999). Ages are reported with one sigma confidence levels from the date of measurement (2019; Table 2).

4. Results

Both the quartz and feldspar ages over-estimate the dune tail age of 10 years by returning ages of between 159 ± 23 and 30 ± 12 years respectively. Age over-estimation was clearly worse for quartz. Whilst it was possible to construct well-constrained SAR growth curves for both quartz and feldspars, the feldspar measurements had a significantly better signal to noise ratio (Fig. 7). To reduce the age over-estimation, two further approaches were taken. Firstly, Ballarini et al. (2007) proposed that improvements determining the age of young quartz samples could be made by shortening the integration intervals taken as signal and subtracting more of the shine-down curve as background. This focusses the measured signal used for D_e estimation on the quartz fast

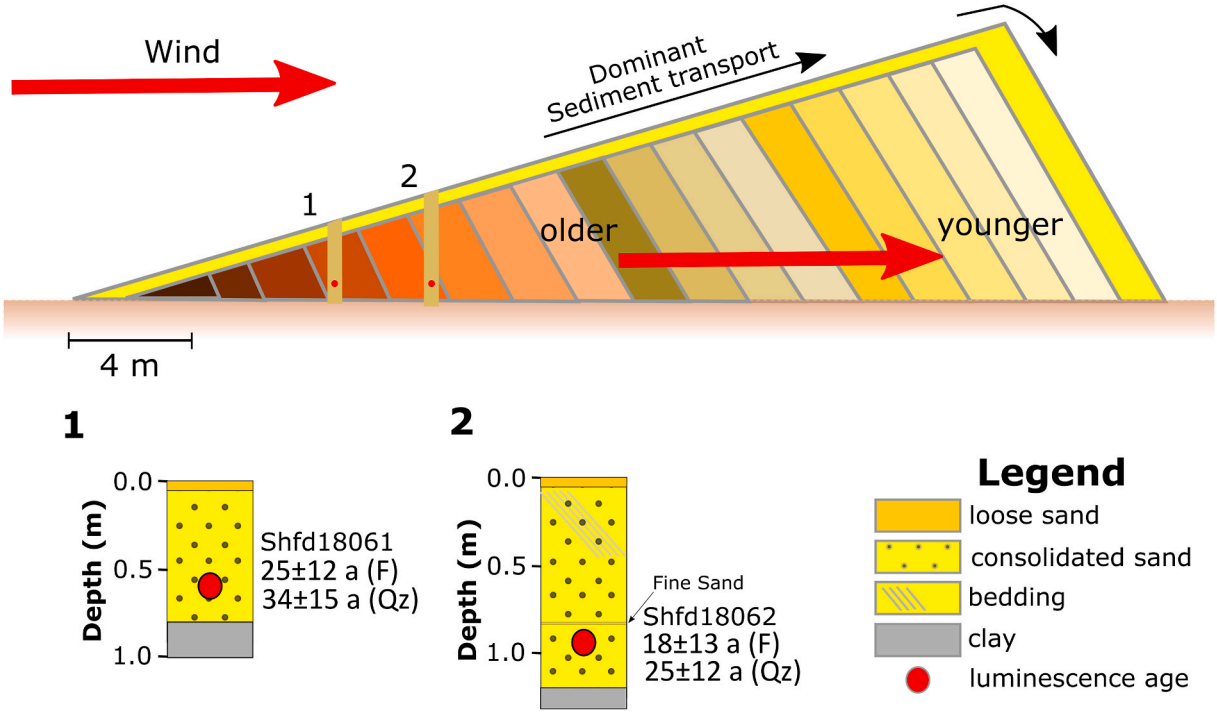

Fig. 6. Upper panel showing schematic of how sediment is deposited on a barchan dune and how as it migrates older material is recycled. Thus, sediments with the oldest age should be found in the tail. Lower panel shows the early background subtracted luminescence age results from the sampled sites in years CE.

Table 2
Luminescence data for Gonghe Basin barchan dune as measured by quartz OSL and feldspar IRSL at the single aliquot level. Overdispersion (OD) given and in parenthesis without outliers. Ages shaded in green are those within one standard error of the satellite derived age of 10 years.

Sample	Labcode	Depth (cm)	Dose Rate (Gy/ka)	n	OD (%)	Late Background subtraction		Revised	
						D_e (Gy)	Age (a)	D_e (Gy)*	Age (a)
Quartz									
Site 1	Shfd18061	0.6	2.398±0.100	23	119 (56)	0.31±0.09	131±37	0.08±0.04	34±15
Site 2	Shfd18062	0.95	2.326±0.098	24	100 (0)	0.37±0.05	159±23	0.06±0.04	25±17
Feldspar									
Site 1	Shfd18061	0.6	3.168±0.099	23	121 (0)	0.10±0.04	30±12	0.08±0.04	25±12
Site 2	Shfd18062	0.95	3.125±0.099	24	105 (0)	0.15±0.06	48±19	0.06±0.04	18±13

* An experimentally derived unbleachable residual level of 0.003Gy was subtracted from all quartz D_e values. Quartz revised D_e values also were calculated using the Early background subtraction method whilst feldspar revised D_e values were calculated using a shorter signal integral to improve the signal to background ratio (see text for details).

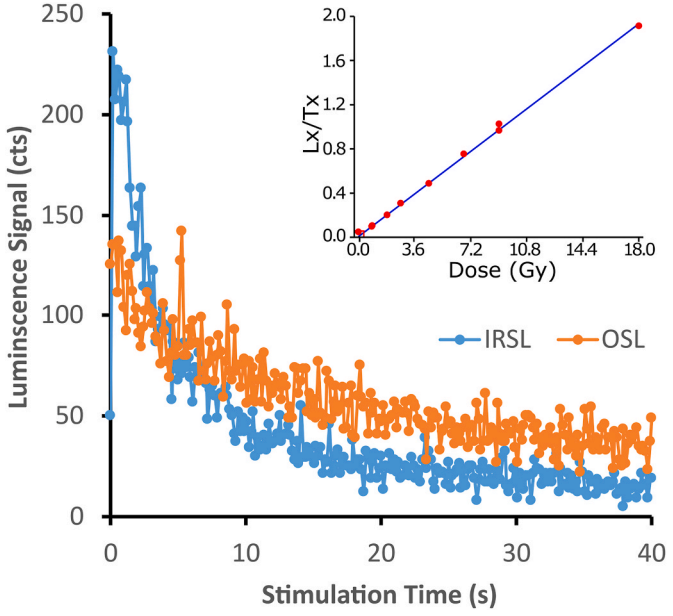

Fig. 7. Example of the luminescence signal for a sample from the Tibetan barchan showing the better signal to noise ratio of feldspar than quartz. Inset shows quartz SAR growth curve showing good linear growth with dose.

component (minimising contributions from unstable medium or slow components; e.g., Brill and Cisternas, 2020). Known as Early Background Subtraction, it was applied to the quartz data in this case study by reducing the signal integral to the first 0.48s of stimulation and subtracting as background all signal for the rest of the shine-down curve (39.52s). Whilst there is no need to avoid slow or medium signal components in the IRSL signal from feldspars, it was observed that by also reducing the signal integral to the first 0.48s of stimulated data it was possible to better encapsulate the small and rapidly decaying IRSL signal (Fig. 7). This improved the signal to background ratio and so was applied to the IRSL data. The second approach was to quantify any unbleachable component as even a small residual D_e could be of significance for young samples which themselves had very small burial D_e values. This was achieved by exposing small quantities of the prepared quartz to 10 days natural day-light before measuring as above. This resulted in a residual of 0.003 Gy which was subtracted from the measured quartz burial D_e values. These modified approaches showed improvement, especially for the quartz results resulting in both quartz and feldspar ages from the same sample agreeing with each other. Quartz OSL returned ages of 34 ± 15 and 25 ± 17 and feldspar IRSL ages of 25 ± 12 and 18 ± 13 for sites 1 and 2 respectively (Table 2). The feldspar age for site 1 and the quartz age for site 2 are close (when errors are considered) to the true burial age of the barchan's tail (10 years) although the errors are large. Overall the feldspar ages appear much closer to the true age of the barchan than those from quartz.

5. Discussion

5.1. Horizontal v vertical sampling

The Storegga data above showed that application of horizontal sampling did provided the correct age irrespective of method or whether measured at the single grain or single aliquot level. Sampling vertically and subsampling it for SA and SG measurements provided a lot more information. However, it appears to have worked less well as individual subsamples had higher OD values, and D_e distributions were more skewed for the SA IRSL. For the latter, even after applying MAM for D_e calculation, age under/over-estimates were returned. Overall, quartz SA OSL subsample ages from the vertical core ranged from 5280 to 9230 years with a standard deviation of 1180 years (Table 1). This compares to 6900–10,480 years and 1110 years for the feldspar SA IRSL and 7290–13,170 years and 1580 years for the feldspar SG pIRIR (Fig. 3). As the tsunami event being dated was a single event in time (<1 day), variability in the subsamples from the vertical core cannot be attributed to real age differences down the core in this instance. Partial bleaching is also ruled out due to the agreement of feldspar and quartz ages, low OD values and normal D_e distributions at the SA level in the horizontal sample. For other studies with different depositional contexts both of these issues could add complexity to understanding data.

In part, more consistent results with horizontal sampling conforms to expectations as it should have ensured lower sediment variability. By sampling in the centre of the tsunami unit (between 6 and 9 cm) only sediment from wave 2, which was the main tsunami wave was collected (Fig. 3; Bateman et al., 2021). Also, in preparing the sample as one, differences in D_e (due to beta heterogeneity for example) would have been better homogenised so that the SA aliquots measured were more likely to be consistent. In contrast, in the vertical core some subsamples came from waves 1 and 3 with potentially different sediment sources, grain size distributions and bleaching histories (Fig. 3). Perhaps more pertinently, by subsampling and separately preparing subsamples from the vertical core any underlying D_e variability was retained and was measured in these subsamples.

In the vertical core from the tsunami deposit the quartz SA showed under-estimation of age for some subsamples (Fig. 3). Similar under-estimation of SA quartz ages has been reported elsewhere and attributed to anomalous fading of quartz (e.g., Feng et al., 2022). In the current study, quartz sample purity was checked and passed an IR ratio

test (as per Duller, 2003) and measurement was with an additional IR wash prior to all OSL measurements (as per Banerjee et al., 2001). Despite this, some aliquots still showed signs of feldspar contamination with a positive relationship between IRSL signal (as measured during the IR wash) and OSL signal post wash (Fig. 8A). In addition to any anomalous fading, incomplete removal of the faster accumulating feldspar signal would lead to an erroneously high gradient on the SAR growth curve when regeneration points were measured and therefore an under-estimation of the true quartz D_e. The difficulty in extracting pure quartz and the on-going presence of feldspar inclusions reflect that the tsunami sediment was eroded from feldspar rich local geology (Bateman et al., 2021). One approach to resolve the quartz SA under-estimation would have been to measure and correct for fading, although precisely establishing fading rates of <1.5% per decade is difficult (Feng et al., 2022). An alternative would be to remove the contaminating feldspars from the quartz prior to measurement. Repeating HF treatment until no IRSL signal was measurable could have been applied (as per del Río et al., 2019 for example) but calculating the actual grain size removed for dose-rate purposes becomes more challenging as increased HF etching is likely to preferentially remove material along cleavage planes and other lines of weakness in grains. Additionally, if the feldspars are inclusions within the quartz this approach will not work without losing most of the quartz as well. A final approach would be to remove the feldspar derived luminescence signal prior to OSL measurement. SA OSL measurements of the horizontal sample without any IR wash returned an age >40% younger than the true age. So, although the IR wash included in the SAR measurements in the current study made a positive impact, it would appear that 40s of IRSL at 50 °C was insufficient in duration to remove all the feldspar signal from all the aliquots. As shown with the multiple and extended IR stimulations at various elevated temperatures carried out during pIRIR protocols (e.g., Rhodes, 2015), effective reduction of IRSL signal to background in feldspars is hard to achieve requiring prolonged stimulation times. We therefore recommend that where feldspar inclusions are suspected the quartz OSL signal maybe best cleaned using much longer IR washes (e.g., 300s) within SAR.

The vertical core subsample data variability from the tsunami deposit also probably reflects beta heterogeneity. The short pathway of beta radiation (1–2 mm) means different grains will each receive a different beta-dose if the sources of the beta dose are not uniformly spread through the deposits but are clustered (e.g. Guérin et al., 2012). A more extreme example of this was demonstrated with autoradiography by Brill et al. (2017) where dated quartz and feldspars were embedded in poorly sorted mixtures of shell hash which caused micro dose-rate variability. In the current study, beta-dose rates were averaged over 1 cm subsamples but this may still not accurately reflect the actual beta-dose received at the grain level. Fig. 3 shows that the beta-dose down core is variable. The noted presence of mottling of the sand within the tsunami unit (Fig. 1C) may also be indicative of an underlying complex distribution of dose emitting elements. As the external beta dose-rate for feldspars is a lower proportion of the total dose rate, variability attributable to beta heterogeneity for the feldspar data should be lower. This (and the feldspar contamination of quartz discussed above) may explain the lower variability of the feldspar SA data compared to quartz from the vertical subsamples.

In summary, horizontal sampling was straight forward and produced the correct ages. Analysis required no D_e analysis beyond application of CAM and the same external gamma and beta dose could be applied to all aliquots/grains. Some of the complexities of the vertical core results were due to the measurements having been made on small subsamples which have suffered from beta-heterogeneity. Had the vertical core been prepared as one sample this may not have been apparent in the resultant data. If all subsamples had not been measured but only one randomly selected, the true burial age may not have been achieved even when subsample specific beta-dose were calculated and, in the case of feldspar SA measurements, further statistical analysis and the use of MAM were employed. Thus, for this case study no clear advantage in terms of final age determination was seen in either sampling approach although more care had to be taken in determining the beta dose rate for the vertical core due to beta heterogeneity. Had the unit accumulated over a longer time horizontal sampling would have been better and we recommend this where at all possible.

5.2. Single aliquot v single grain

Both SA and SG measurements were only measured on feldspars from the tsunami deposit. Whilst the down core D_e standard deviation between subsamples for the pIRIR SG data was the highest of all three approaches undertaken (see above), this was levered by a single subsample at 7 cm depth which gave a large age over-estimation (Table 1). Excluding this value reduced the standard deviation of ages between subsamples to only 480 years making this data from the vertical core both the most consistent and closest to true age of the methods measured. Thus, for pIRIR SG measurements on the vertical core, if all subsamples had not been measured but only one randomly selected, it is more than likely that the true burial age would have been achieved. This approach, in being measured at elevated temperatures, should also have minimise any anomalous fading. A small number of aliquots measured with IRSL at 50 °C were observed to return anomalously low D_e values which may indicate that a small proportion of grains within the tsunami deposit did suffer from fading (Fig. 4). Additionally, by being at the SG level, the pIRIR data also allowed better exclusion of saturated grains. Whilst they represented only a low proportion of grains, the averaging effects of measuring simultaneously 90 grains per aliquot for SA precluded their identification and exclusion but would have added to

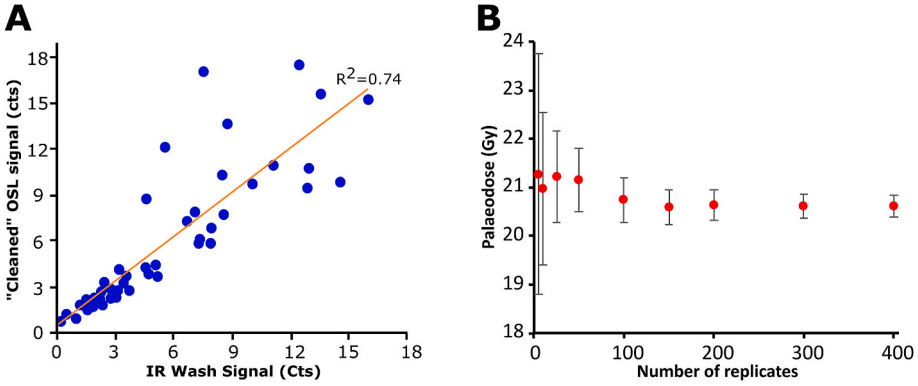

Fig. 8. (A) Luminescence data measured on single aliquots of quartz showing that even after an IR wash those aliquots with a high IR response still had a high OSL response. This is taken to be indicative of feldspar inclusions within the quartz grains. (B) Bootstrapped CAM palaeodoses values for different replicate numbers from the pIRIR SG dataset. Uncertainty derived from rerunning bootstrapping 5 times.

sample D_e variability between aliquots and between subsamples from the vertical core. A small number of feldspar SA aliquots with very high D_e values were observed and may be as a result of this (Fig. 4). On this basis, and in common with a number of recent studies, we recommend single grain measurement of feldspars with pIRIR.

5.3. Number of replicates to be measured

Despite issues highlighted above, by combining all the D_e data from the vertical Storegga tsunami subsamples, applying MAM to the feldspar data, and applying the bulk external beta dose rate for the tsunami sand unit correct ages were obtained from the vertical sample for feldspars (SA and SG) and quartz (SA; Table 1). From this we can say that when the D_e replicate population measured was large enough, any aliquots/grains that had issues were in sufficiently low numbers not to have a leverage effect on the final extracted D_e value use for age calculation purposes. In this case, the most affected grains or aliquots on such large datasets become outlier values. Many luminescence studies creating chronological datasets typically derive ages from up to 48 aliquot replicates (mostly much less) or, in the case of single grain measurements, <100 grains which meet the appropriate quality assurance criteria for D_e acceptance. Rodnight (2008) recommended for SA measurement of poorly bleached samples 50 D_e replicates should be measured. This present study shows that, even in well-bleached sediment such as the tsunami sand, this number of replicates is too low. Bootstrapping different numbers of D_e replicates from the tsunami deposit IRSL SG dataset was undertaken (Fig. 8B). Statistically, when uncertainties are considered, all the resultant D_e values based on different numbers of replicates are indistinguishable. However, an observation can be made. With 150+ replicates the extracted D_e remains similar and uncertainties reduce to <2% (uncertainties are 12% when n = 5 and 4% when n = 25). An alternative, and more positive way of putting this, is that measuring larger numbers of replicates can reduce uncertainties, obviate the necessity of modelling micro-scale beta dose variations (Chauchan and Singhvi, 2011; Guérin et al., 2012, 2015) and help statistical analysis to exclude aliquots/grains where only minor fading, feldspar inclusions and partial bleaching occurred. Brill et al. (2018) reported cyclone and tsunami sediment ages where D_e scatter was attributed to both partial bleaching and micro-dosimetry but as replicate numbers were high (mean = 144 grains) this allowed appropriate extraction of the burial D_e and good age agreement with historical sources of age. We suggest routinely basing ages on a larger number of palaeodose replicates (>150) would be beneficial especially in depositional environments where grain bleaching prior to burial may have been variable.

5.4. Dating young samples

The Tibet barchan samples measured at the SA level using with SAR led to age-over-estimations. This is particularly the case for quartz. If the feldspars had suffered from anomalous fading (not tested in this study) then correction for this would have increased their age over-estimation. For example, with a g-value of 5%/decade the feldspar ages would have been 8–11 years older. Further steps were required to produce ages within error of the true age. For quartz application of the early background subtraction (EBG) method was significant. This, in reducing any contributions from medium and slow OSL signal components, lowered sample D_e values by 73–83% and therefore greatly improved true age estimation. Also for quartz, whilst the measured unbleachable residual was small (0.003Gy), relative to D_e values measured in the samples (0.06–0.08 Gy) it represented 3–4% of measured D_e and therefore proved worth removing before age calculation. For feldspar measurements, focussing the signal integral used to plot growth curves to target only the initial high IRSL signal lowered D_e values by 17–58% and again improved true age estimation. Quartz SA OSL as well as SA and SG IRSL and pIRIR was applied to young (<500 years old) earthquake related samples in a study from Chile (Brill and Cisternas 2020). Here, whilst EBG improved OSL ages, both OSL and IRSL, just like this study, also led to age over-estimation when compared to control ages. Improved agreement with control ages was shown for pIRIR results.

Overall feldspar ages are closest to true burial age. This reflects that IRSL signal accumulates more rapidly than the OSL signal from quartz due to both the higher feldspar dose-rate as a result of the internal dosing from potassium and the known higher sensitivity (brightness per unit dose) of feldspars when compared to quartz. For young samples in what should be well bleached depositional contexts such as dunes, any disadvantages of feldspars as a dosimeter (slower bleaching prior to burial and anomalous fading) may be outweighed by being able to measure their IRSL signal more accurately and precisely. As investigated by Osunkwor and De Witt (2021), the small but persistent remaining age over-estimation for both quartz and feldspar may be due to irradiation cross-talk during measurement in the Risø automated TL/OSL reader and would be worth further investigation. Additionally, Brill and Cisternas (2020) showed improvements in age accuracy with ultra-small (1 mm diameter) aliquots and single grain measurements, and this may also be worth consideration providing the naturally acquired signal is bright enough to be measured at these levels. In summary, based on this study, for dating very young samples use of feldspar IRSL with data analysis modified to maximising the signal to noise ratio is recommended.

6. Conclusions

This study illustrates that it matters how and from where samples are collected in relation to the event of interest. Whilst vertical coring maybe unavoidable in some instances, consideration should be given to how much time is being averaged by a vertical sample and avoided if possible.

As often luminescence sample preparation is conservative producing more prepared material than is ultimately needed, subsampling and preparation of a smaller amount of material from the middle of the core may reduce any impacts of the vertical sampling. However, as shown here, measurement of very small subsamples, especially if in complex depositional and dose rate scenario's, maybe more prone to inaccuracies when measured at the SA level. Ideally, the level of D_e measurement and dose-rate determination should match to avoid knowing the D_e at individual grain level but only an average dose-rate of the whole unit. In this study SG pIRIR measurements with beta-dose rates calculated for each subsample produced the least variable and most accurate age estimates for the Storegga tsunami sediment.

In addition, or as an alternative to the above, increasing D_e replicates may be able to overcome minor beta heterogeneity, bleaching and contamination issues by resolving them sufficiently that they can be dealt with by statistical analysis of the D_e data. Increasing the number of D_e replicates can also improve both accuracy/precision and we recommend of measurement of >150 D_e replicates for each sample as a consequence.

In both case studies application of SAR D_e measurements without modification and/or application of additional data analysis steps may have led to misleading age determination had the true age not been known. For the Storegga samples, detection and removal of signal from feldspar contamination in quartz samples was needed. In the vertical core careful consideration was required of changes in beta dose-rate down core and feldspar SA data required D_e analysis with MAM due to skewed D_e distributions. The latter was not required for the SG pIRIR measurements, and these performed the best out of the approaches undertaken. For the Tibetan barchan, maximising the signal to noise ratio on such young samples was the key to avoiding significant age over-estimation and feldspar IRSL measurements appeared to perform better than quartz OSL. Overall, we conclude that luminescence dating has not yet reached a point where it can be undertaken routinely without specialist knowledge.

Declaration of competing interest

The authors declare that they have no known competing financial interests or personal relationships that could have appeared to influence the work reported in this paper.

Acknowledgements

Thanks to Rob Ashurst for preparing luminescence samples and Vanessa Kirkbride from Scottish National Heritage for arranging Montrose site access. Sampling in Gonghe Basin was made possible through the financial support of Prof Lou and the National Natural Science Foundation of China (Grant No. 41771015). Thanks are also extended to the reviewers and Special Issue Editor for their comments on earlier drafts of this manuscript.

References

Aitken, M.J., 1987. Thermoluminescence Dating. Academic Press, Orlando.
Ankjægaard, C., Guralnik, B., Buylaert, J.-P., Reimann, T., Yi, S.W., Wallinga, J., 2016. Violet stimulated luminescence dating of quartz from Luochuan (Chinese loess plateau): agreement with independent chronology up to ~600 ka. Quat. Geochronol. 34, 33–46.
Arnold, L.J., Roberts, R.G., 2009. Stochastic modelling of multi-grain equivalent dose (D_e) distributions: implications for OSL dating of sediment mixtures. Quat. Geochronol. 4, 204–230.
Balescu, S., Lamothe, M., 1994. Comparison of TL and IRSL age estimates of feldspar coarse grains from waterlain sediments. Quat. Sci. Rev. 13, 437–444.
Ballarini, M., Wallinga, J., Wintle, A.G., Bos, A.J.J., 2007. A modified SAR protocol for optical dating of individual grains from young quartz samples. Radiat. Meas. 42, 360–369.
Banerjee, D., Murray, A.S., Bøtter-Jensen, L., Land, A., 2001. Equivalent dose estimation using a single aliquot of polymineral fine grains. Radiat. Meas. 33, 73094.
Bateman, M.D., Catt, J.A., 1996. An absolute chronology for the raised beach and associated deposits at Sewerby, East Yorkshire, England. J. Quat. Sci. 11, 389–395.
Bateman, M.D., Frederick, C.D., Jaiswal, M.K., Singhvi, A.K., 2003. Investigations into the potential effects of pedoturbation on luminescence dating. Quat. Sci. Rev. 22, 1169–1176.
Bateman, M.D., Boulter, C.H., Carr, A.S., Frederick, C.D., Peter, D., Wilder, M., 2007. Detecting Post-depositional sediment disturbance in sandy deposits using optical luminescence. Quat. Geochronol. 2, 57–64.
Bateman, M.D., Carr, A.S., Murray-Wallace, C.V., Roberts, D.L., Holmes, P.J., 2008. A dating intercomparison study on Late Stone Age coastal midden deposits, S. Africa. Geoarchaeology 23, 715–741.
Bateman, M.D., Rushby, G., Stein, S., Ashurst, R.A., Stevenson, D., Jones, J.M., Gehrels, W.R., 2018. Can sand dunes be used to study historic storm events? Earth Surf. Process. Landforms 43, 779–790.
Bateman, M.D., Kinnaird, T.C., Hill, J., Ashurst, R.A., Mohan, J., Bateman, R.B.I., Robinson, R., 2021. Detailing the impact of the Storegga tsunami at Montrose, Scotland. Boreas 50, 1059–1078.
Bondevik, S., Lovholt, F., Harbitz, C., Mangerud, J., Dawson, A.G., Svendsen, J.I., 2005. The Storegga Slide tsunami – comparing field observations with numerical simulations. Mar. Petrol. Geol. 22, 195–208.
Bondevik, S., Stormo, S.K., Skjerdal, G., 2012. Green mosses date the Storegga tsunami to the chilliest decades of the 8.2 ka cold event. Quat. Sci. Rev. 45, 1–6.
Briant, R.M., Bateman, M.D., 2009. Luminescence dating indicates radiocarbon age underestimation in Late Pleistocene fluvial deposits from eastern England. J. Quat. Sci. 24, 916–927.
Brill, D., Klasen, N., Brückner, H., Kruawun, J., Scheffers, A., Kelletat, D., Scheffers, S., 2012. OSL dating of tsunami deposits from Phra THONG Island, Thailand. Quat. Geochronol. 10, 224–229.
Brill, D., May, S.M., Shah-Hosseini, M., Rufer, D., Schmidt, C., Engel, M., 2017. Luminescence dating of cyclone-induced washover fans at Point Lefroy (NW Australia). Quat. Geochronol. 41, 134–150.
Brill, D., Reimann, T., Wallinga, J., Matthias May, S., Engel, M., Riedesel, S., Brückner, H., 2018. Testing the accuracy of feldspar single grains to date late Holocene cyclone and tsunami deposits. Quat. Geochronol. 48, 91–103.
Brill, D., Cisternas, M., 2020. Testing quartz and feldspar luminescence dating to determine earthquake and tsunami recurrence in the area of the giant 1960 Chile earthquake. Quat. Geochronol. 58, 101080.
Bryant, R.G., Baddock, M.C., 2021. Remote sensing of aeolian processes. Ref. Modul. Earth Syst. Environ. Sciences. (in press).
Buylaert, J.P., Jain, M., Murray, A.S., Thomsen, K.J., Thiel, C., Sohbati, R., 2012. A robust feldspar luminescence dating method for Middle and Late Pleistocene sediments. Boreas 41, 435–451.
Chauchan, N., Singhvi, A.K., 2011. Distribution in SAR palaeodoses due to spatial heterogeneity of natural beta dose. Geochronometria 38, 190–198.
Cunningham, A.C., Bakker, M.A.J., van Heteren, S., van der Valk, B., van der Spek, A.J. F., Schaart, D.R., Wallinga, J., 2011. Extracting storm-surge data from coastal dunes for improved assessment of flood risk. Geology 39, 1063–1066.
Dawson, A.G., Long, D., Smith, D.E., 1988. The Storegga Slide: evidence from eastern Scotland for a possible tsunami. Mar. Geol. 82, 271–276.
del Río, I., Sawakuchi, A.O., Gonzalez, G., 2019. Luminescence dating of sediments from central Atacama Desert, northern Chile. Quat. Geochronol. 53, 101002.
Duller, G.A.T., 2003. Distinguishing quartz and feldspar in single grain luminescence measurements. Radiat. Meas. 37, 161–165.
Feng, Y., Hou, Y., Zhang, J., Yang, N., Cai, Y., Yang, F., Gu, J., Long, H., 2022. Timing of Holocene lake highstands around Dawa Co in inner Tibetan Plateau: comparison of quartz and feldspar luminescence dating with radiocarbon age. Quat. Geochronol. 69, 101267.
Fuchs, M., Owen, L.A., 2008. Luminescence dating of glacial and associated sediments: review, recommendations and future directions. Boreas 37, 636–659.
Galbraith, R.F., Roberts, R.G., Laslett, G.M., Yoshida, H., Olley, J.M., 1999. Optical dating of single and multiple grains of quartz from Jinmium rock shelter, northern Australia, Part I: experimental Design and Statistical Models. Archaeometry 41, 339–364.
Guérin, G., Mercier, N., Adamiec, G., 2011. Dose-rate conversion factors: update. Ancient TL 29, 5–8.
Guérin, G., Mercier, N., Nathan, R., Adamiec, G., Lefrais, Y., 2012. On the use of the infinite matrix assumption and associated concepts: a critical review. Radiat. Meas. 47, 778–785.
Guérin, G., Jain, J., Thomsen, K.J., Murray, A.S., Mercier, N., 2015. Modelling dose rate to single grains of quartz in well-sorted sand samples: the dispersion arising from the presence of potassium feldspars and implications for single grain OSL dating. Quat. Geochronol. 27, 52–65.
Ito, K., Tamura, T., Hasebe, N., Itono, T., Nakamura, T., Arai, S., Ogata, M., Kashiwaya, K., 2015. Comparison of luminescence dating methods on lake sediments from a small catchment: example from Lake Yogo, Japan. In: Kashiwaya, K., Shen, J., Kim, J., Yong, J. (Eds.), Earth Surface Processes and Environmental Changes in East Asia. Springer, p. pp321.
Ishizawa, T., Goto, K., Yokoyama, Y., Goff, J., 2020. Dating tsunami deposits: present knowledge and challenges. Earth Sci. Rev. 200, 102971.
Kim, M.J., Jung, B.G., Kim, S.Y., Hong, D.G., 2013. Comparison of OSL and 14C dates estimated from paleolithic paleosol of the Suheol-ri site in Cheonan, Korea. Mediterr. Archaeol. Archaeometry 13, 117–126.
Lamothe, M., Balescu, S., Auclair, M., 1994. Natural IRSL intensities and apparent luminescence ages of single feldspar grains extracted from partially bleached sediments. Radiat. Meas. 23, 555–561.
Leighton, C.L., Bailey, R.M., Thomas, D.S.G., 2013. The utility of desert sand dunes as Quaternary chronostratigraphic archives: evidence from the northeast Rub'al Khali. Quat. Sci. Rev. 78, 303–318.
Luo, W.Y., Wang, Z.Y., Shao, M., Lu, J.F., Qian, G.Q., Dong, Z.B., Bateman, M.D., 2019a. Historical evolution and controls on mega-blowouts in north-eastern Qinghai-Tibetan Plateau, China. Geomorphology 329, 17–31.
Luo, W.Y., Wang, Z.Y., Lu, J.F., Yang, L.H., Qian, G.Q., Dong, Z.B., Bateman, M.D., 2019b. Mega-blowouts in Qinghai–Tibet plateau: morphology, distribution and initiation. Earth Surf. Process. Landforms 44, 449–458.
Lou, W., Shai, M., Che, X., Hesp, P., Bryant, R.G., Yan, C., Xing, Z., 2020. Optimization of UAVs-SfM data collection in aeolian landform morphodynamics: a case study from the Gonghe Basin, China. Earth Surf. Process. Landforms 45, 3293–3312.
Mahan, S., DeWitt, R., 2019. Principles and history of luminescence dating. In: Bateman, M.D. (Ed.), The Handbook of Luminescence Dating. Whittles Publishing, p. 416.
Murray, A.S., Funder, S., 2003. Optically stimulated luminescence dating of a Danish Eemian coastal marine deposits: a test of accuracy. Quat. Sci. Rev. 22, 1177–1183.
Murray, A.S., Wintle, A.G., 2000. Luminescence dating of quartz using an improved single aliquot regenerative-dose protocol. Radiat. Meas. 32, 57–73.
Murray, A.S., Wintle, A.G., 2003. The single aliquot regenerative dose protocol: potential for improvements in reliability. Radiat. Meas. 37, 377–381.
Nanson, G.C., Young, R.W., 1986. Comparison of thermoluminescence and radiocarbon age-determinations from late-Pleistocene alluvial deposits near Sydney, Australia. Quat. Res. 27, 263–269.
Osunkwor, E., De Witt, R., 2021. Beta dose rate reduction for the built-in $^{90}Sr/^{90}Y$ sources of Risø TL/OSL automated readers. Ancient TL 39, 18–27.
Prescott, J.R., Hutton, J.T., 1994. Cosmic ray contributions to dose rates for luminescence and ESR dating: large depths and long-term time variations. Radiat. Meas. 2 (3), 497–500.
Prescott, J.R., Williams, F.M., Hunt, C.D., 2007. Comparison of TL multiple aliquot, single grain GLSL SAR and C-14 ages for the Puritjarra, Australia, rock shelter. Quat. Geochronol. 2, 344–349.
Qi, Y.H., Pan, M.H., Hao, Z.W., Yang, A-n, Xue, W-x, 2021. Variations in aeolian landform patterns in the Gonghe Basin over the last 30 years. J. Mt. Sci. 18.
Rhodes, E.J., 2015. Dating sediments using potassium feldspar single-grain IRSL: initial methodological considerations. Quat. Int. 362, 14–22.
Reimann, T., Román-Sánchez, A., Vanwalleghem, T., Wallinga, J., 2017. Getting a grip on soil reworking – single-grain feldspar luminescence as a novel tool to quantify soil reworking rates. Quat. Geochronol. 42, 1–14.
Roberts, R.G., Galbraith, R.F., Olley, J.M., Yoshida, H., Laslett, G.M., 1999. Optical dating of single and multiple grains of quartz from Jinmium rock shelter, Northern Australia: Part II, Results and implications. Archaeometry 41, 365–395.
Rodnight, H., Duller, G.A.T., Wintle, A.G., Tooth, S., 2006. Assessing the reproducibility and accuracy of optical dating of fluvial deposits. Quat. Geochronol. 1, 109–120.
Rodnight, H., 2008. How many equivalent dose values are needed to obtain a reproducible distribution? Ancient TL 26, 3–9.

Smedley, R.K., Buylaert, J.-P., Ujvari, G., 2019. Comparing the accuracy and precision of luminescence ages for partially-bleached sediments using single grains of K-feldspar and quartz. Quat. Geochronol. 53, 101007.
Smith, M.A., Prescott, J.R., Head, M.J., 1997. Comparison of 14C and luminescence chronologies at Puritjarra rock shelter, central Australia. Quat. Sci. Rev. 16, 299–320.
Smith, D.E., Shi, S., Cullingford, R.A., Dawson, A.G., Dawson, S., Firth, C.R., Foster, I.D. L., Fretwell, P.T., Haggart, B.A., Holloway, L.K., Long, D., 2004. The holocene Storegga slide tsunami in the United Kingdom. Quat. Sci. Rev. 23, 2291–2321.
Shtienberg, G., Yasur-Landau, A., Norris, R.D., Lazar, M., Rittenour, T.M., Tamberino, A., Gadol, O., Cantu, K., Arkin-Shalev, E., Ward, S.N., Levy, T.E., 2020. A Neolithic mega-tsunami event in the eastern Mediterranean: prehistoric settlement vulnerability along the Carmel coast, Israel. PLoS One 15, e0243619.
Song, Y., Lai, Z., Li, Y., Chen, T., Wang, Y., 2015. Comparison between luminescence and radiocarbon dating of late quaternary loess from the Ili basin in central Asia. Quat. Geochronol. 30, 405–410.
Vandenberghe, D., Kasse, C., Hossain, S.M., de Corte, F., van den Haute, P., Fuchs, M., Murray, A.S., 2004. Exploring the method of optical dating and comparison of optical and 14C ages of Late Weichselian coversands in the southern Netherlands. J. Quat. Sci. 19, 73–86.
Wagner, B., Bennike, O., Cremer, H., Klug, M., 2010. Late quaternary history of the Kap Mackenzie area, northeast Greenland. Boreas 39, 492–504.
Wallinga, J., Murray, A.S., Wintle, A., 2000. The single-aliquot regenerative-dose (SAR) protocol applied to coarse-grain feldspar. Radiat. Meas. 32, 529–533.
Wallinga, J., Murray, A.S., Duller, G.A.T., Tornqvist, T.E., 2001. Testing optically stimulated luminescence dating of sand-sized quartz and feldspar from Fluvial deposits. Earth Planet Sci. Lett. 193, 617–630.